THE JOURNAL OF CELL BIOLOGY

Tim23–Tim50 pair coordinates functions of translocators and motor proteins in mitochondrial protein import

Yasushi Tamura,[1] Yoshihiro Harada,[1] Takuya Shiota,[1] Koji Yamano,[1] Kazuaki Watanabe,[1] Mihoko Yokota,[1] Hayashi Yamamoto,[1] Hiromi Sesaki,[2] and Toshiya Endo[1]

[1]Department of Chemistry, Graduate School of Science, Nagoya University, Chikusa-ku, Nagoya 464-8602, Japan
[2]Department of Cell Biology, The Johns Hopkins University School of Medicine, Baltimore, MD 21205

Mitochondrial protein traffic requires coordinated operation of protein translocator complexes in the mitochondrial membrane. The TIM23 complex translocates and inserts proteins into the mitochondrial inner membrane. Here we analyze the intermembrane space (IMS) domains of Tim23 and Tim50, which are essential subunits of the TIM23 complex, in these functions. We find that interactions of Tim23 and Tim50 in the IMS facilitate transfer of precursor proteins from the TOM40 complex, a general protein translocator in the outer membrane, to the TIM23 complex. Tim23–Tim50 interactions also facilitate a late step of protein translocation across the inner membrane by promoting motor functions of mitochondrial Hsp70 in the matrix. Therefore, the Tim23–Tim50 pair coordinates the actions of the TOM40 and TIM23 complexes together with motor proteins for mitochondrial protein import.

Introduction

Normal eukaryotic cell functions rely on dedicated systems of protein traffic control that ensure correct assembly of specific sets of proteins in each membrane-bounded compartment or organelle (Schatz and Dobberstein, 1996). Mitochondria are two-membrane bounded organelles consisting of ~1,000 different proteins, most of which are synthesized in the cytosol as precursor proteins, imported into mitochondria, and sorted to one of the four subcompartments, the outer membrane, intermembrane space (IMS), inner membrane, and matrix. Protein import and sorting are mediated by membrane protein assemblies called translocators, including the TOM40 and TOB/SAM complexes in the outer membrane and the TIM23 and TIM22 complexes in the inner membrane (Koehler, 2004; Kutik et al., 2007; Neupert and Herrmann, 2007). These translocators are not tightly linked to each other, but instead cooperate dynamically to pass precursor proteins onto each other, thereby achieving precise as well as efficient protein delivery to their destinations (Endo et al., 2003; Kutik et al., 2007). The TOM40 complex is the entry site for most mitochondrial proteins, and after translocation through the TOM40 complex, protein sorting pathways branch out for different intramitochondrial locations. Mitochondrial precursor proteins with an N-terminal cleavable presequence use the TIM23 complex to reach the matrix or inner membrane. Presequence-less polytopic membrane proteins including carrier proteins use the TIM22 complex to be inserted into the inner membrane.

Translocation of presequence-containing proteins requires cooperation of the TOM40 complex, TIM23 complex, and import motor proteins in the matrix. Presequences are first recognized by the general import receptor Tom20 of the TOM40 complex on the mitochondrial surface, and then move through the Tom40 channel to reach the trans site for presequence binding, which consists of Tom40, Tom22, and Tom7 on the IMS side of the outer membrane (Endo and Kohda, 2002; Esaki et al., 2004). After crossing the outer membrane, precursor proteins are transferred to the TIM23 complex and sorted to the matrix or inner membrane. Transfer of presequence-containing proteins

Correspondence to Toshiya Endo: endo@biochem.chem.nagoya-u.ac.jp

Y. Tamura's present address is Dept. of Cell Biology, The Johns Hopkins University School of Medicine, Baltimore, MD 21205.

H. Yamamoto's present address is Dept. of Cell Biology, National Institute for Basic Biology, Myodaiji, Okazaki 444-8585, Japan.

Abbreviations used in this paper: BPA, benzoylphenylalanine; DHFR, mouse dihydrofolate reductase; IMS, intermembrane space; MMC, mtHsp70-associated motor and chaperone; mtHsp70, mitochondrial Hsp70; PK, proteinase K.

© 2009 Tamura et al. This article is distributed under the terms of an Attribution–Noncommercial–Share Alike–No Mirror Sites license for the first six months after the publication date (see http://www.jcb.org/misc/terms.shtml). After six months it is available under a Creative Commons License (Attribution–Noncommercial–Share Alike 3.0 Unported license, as described at http://creativecommons.org/licenses/by-nc-sa/3.0/).

Downloaded from http://rupress.org/jcb/article-pdf/184/1/129/1562529/jcb_200808068.pdf by guest on 09 February 2026

The Rockefeller University Press $30.00
J. Cell Biol. Vol. 184 No. 1 129–141
www.jcb.org/cgi/doi/10.1083/jcb.200808068

from the trans site of the TOM40 complex to the TIM23 complex was proposed to be facilitated by (a) the receptor functions of the TIM23 complex specific for presequences (Bauer et al., 1996; Komiya et al., 1998; Yamamoto et al., 2002; Mokranjac et al., 2003), (b) recruitment of the TIM23 complex to the mitochondrial contact sites, where the outer and inner membranes are closely apposed and protein translocation across the two membranes takes place (Donzeau et al. 2000; Vogel et al., 2006), and (c) recruitment of the TIM23 complex to the TOM40 complex by their possible transient interactions (Chacinska et al., 2005; Mokranjac et al., 2005). Tim50 of the TIM23 complex is the first component to receive the translocating precursor protein from the TOM40 complex at the inner membrane (Yamamoto et al., 2002; Mokranjac et al., 2003).

The presequence is then translocated across the inner membrane through the Tim23(-Tim17) channel, depending on the membrane potential across the inner membrane ($\Delta\Psi$; Truscott et al., 2001; Meinecke et al., 2006; Alder et al., 2008b). Subsequent translocation and unfolding of the matrix-targeted precursor protein is driven by the import motor mitochondrial Hsp70 (mtHsp70) or Ssc1p in yeast, which binds to and dissociates from the incoming polypeptide segment at the outlet of the TIM23 channel upon ATP hydrolysis (Neupert and Brunner, 2002; Yamano et al., 2008). mtHsp70 functions in cooperation with partner proteins, mtHsp70-associated motor and chaperone (MMC) proteins, that facilitate protein import into the matrix. MMC proteins include Tim44, Tim14/Pam18, Tim16/Pam16, and Pam17 as subunits of the TIM23 complex and Yge1p/Mge1p and Tim15/Zim17/Hep1 in the matrix. Tim14 is a J-protein that forms a complex with a J-like protein Tim16 and stimulates ATPase activity of mtHsp70. Tim44 directly interacts with the translocating polypeptide and both Tim44 and Pam17 (van der Laan et al., 2005) link Tim14–Tim16 to the TIM23 complex. Translocation of the inner membrane sorted proteins with a hydrophobic sorting signal after the matrix-targeting signal in the presequence is arrested at the inner membrane by the interactions of the sorting signal part with the TIM23 complex and is released laterally into the inner membrane (Glick et al., 1992; Esaki et al., 1999).

Although the IMS domains of Tim23 and Tim50 interact with each other (Geissler et al., 2002; Yamamoto et al., 2002; Alder et al., 2008a), precise roles of those interactions in mitochondrial protein import remain unclear. We thus generated yeast strains with Tim23 or Tim50 mutants that would deteriorate Tim23–Tim50 interactions. Systematic analyses of those mutants revealed that Tim23–Tim50 interactions in the IMS are essential for both the initial and late steps of protein translocation through the TIM23 complex. On the basis of the obtained results, we propose a model for protein translocation across and insertion into the inner membrane via the TIM23 complex in which the Tim23–Tim50 pair in the IMS plays central and multiple roles.

Results

Mutations in the IMS domain of Tim23 cause defective cell growth

The IMS domains of both Tim23 and Tim50 (residues 1–101 and 133–476, respectively) are indispensable and interact with each other likely through their predicted coiled-coil regions (Bauer et al., 1996; Geissler et al., 2002; Yamamoto et al., 2002). To assess the roles of Tim23–Tim50 interactions in the IMS, we systematically introduced mutations in the predicted coiled coil and its flanking regions of Tim23 to disrupt its possible interactions with Tim50 and tested their effects on yeast cell growth. Among them, we observed growth defects for the yeast strains that have Leu→Ser mutations at positions 64, 71, and/or 78 of Tim23, which are expected to form a hydrophobic side of the coiled coil for protein–protein interactions (Fig. 1 A). *tim23* mutant strains with the L71S mutation (*tim23-71*), but not L64S (*tim23-64*) or L78S (*tim23-78*) alone, showed growth defects at elevated temperature (Fig. 1 B). The L78S mutation showed synthetic growth defects with L71S (*tim23-71,78*), and the L64S mutation showed those with L71,78S (*tim23-64,71,78*) (Fig. 1 B), whereas the *tim23* mutant with five mutations at residues 60–64 (*tim23-60-64*) did not cause any growth defects. The L68S and L73S mutations also showed synthetic growth defects with the L71,78S mutation (*tim23-68,71,78* and *tim23-71,73,78* in Fig. 1 B). In contrast, although negative charges in the IMS domain of Tim23 were suggested to be important for its receptor function for positively charged presequences (Bauer et al., 1996; Komiya et al., 1998), the *tim23* mutant with replacement of four negatively charged residues at positions 72, 74, 75, and 76 with positively charged Lys (*tim23-4K*) did not cause obvious growth defects (Fig. 1 B).

Mitochondria with mutations in the IMS domain of Tim23 are defective in protein import

We conducted in vitro protein import into mitochondria with Tim23 containing mutations at positions 64, 71, and/or 78. The mitochondria isolated from the *tim23-71,78* and *tim23-64,71,78* mutants, which show strong growth defects, exhibited the normal levels of translocator components and of $\Delta\Psi$, which is essential for protein import via the TIM23 complexes (Fig. 1, C and D). We first analyzed import of radiolabeled matrix-targeted precursor proteins with an N-terminal presequence, i.e., pSu9–mouse dihydrofolate reductase (DHFR), a fusion protein between the presequence of F_0-ATPase subunit 9 and DHFR, a precursor to mitochondrial Hsp60 (pHsp60), and $pb_2(167)\Delta19$-DHFR and $pb_2(220)\Delta19$-DHFR, the first 167 and 220 residues of the yeast cytochrome b_2 precursor with deletion of the 19-residue inner membrane–sorting signal, respectively, fused to DHFR. Import of those proteins via the TIM23 complex with the aid of the import motor machinery comprising mtHsp70 and MMC proteins was retarded significantly for *tim23-71*, *tim23-71,78*, and *tim23-64,71,78* mitochondria or moderately for *tim23-64* and *tim23-78* mitochondria as compared with wild-type mitochondria (Fig. 2 and Fig. S1 A, available at http://www.jcb.org/cgi/content/full/jcb.200808068/DC1).

We next analyzed import of inner membrane–sorted proteins. Import of the presequence-containing fusion proteins $pb_2(167)$-DHFR and $pb_2(220)$-DHFR, the first 167 and 220 residues of the yeast cytochrome b_2 precursor fused to DHFR, respectively, via the TIM23 complex was retarded for *tim23-71*,

Downloaded from http://rupress.org/jcb/article-pdf/184/1/129/1562529/jcb_200808068.pdf by guest on 09 February 2026

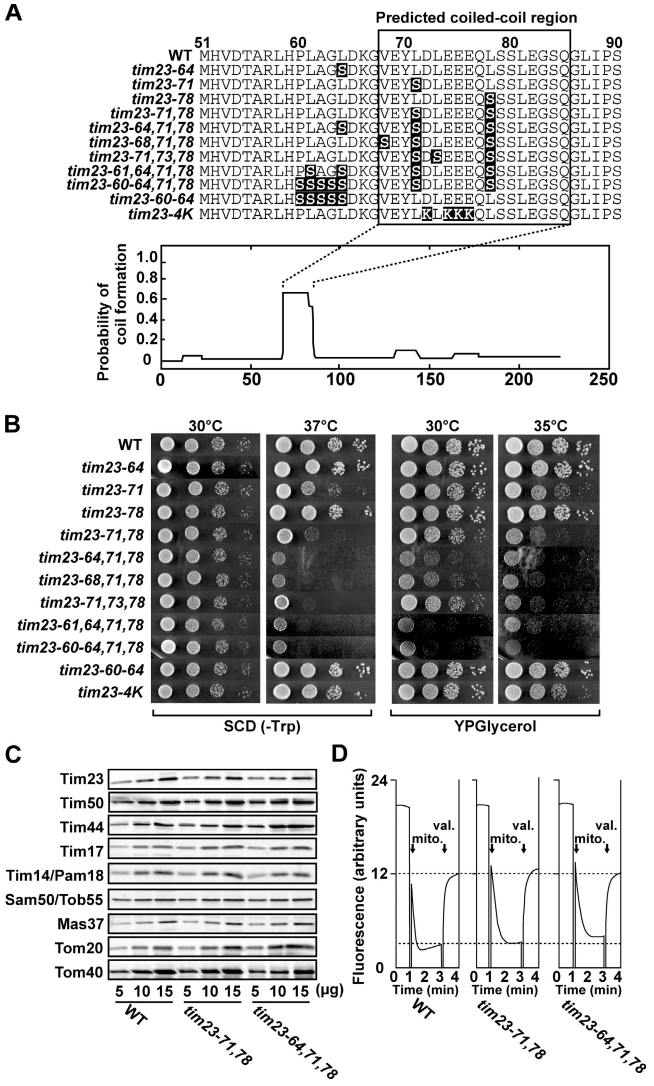

Figure 1. **Tim23 mutants with mutations in the coiled-coil region in the IMS.** (A) Amino acid sequences of the IMS domains of Tim23 mutants in *tim23* mutant strains (top) and coiled-coil regions in Tim23 (bottom) predicted by COILS (http://www.ch.embnet.org/software/COILS_form.html). Mutation points are shown in black. (B) Serial dilutions of *tim23* mutant cells were plated on SCD (−Trp) and YPGlycerol and grown at the indicated temperature for 2 and 3 d, respectively. (C) Mitochondria were isolated from wild-type control (WT) and *tim23* mutant cells grown at 30°C. Indicated amounts of mitochondrial proteins were analyzed for indicated proteins by SDS-PAGE followed by immunoblotting. (D) $\Delta\Psi$ of wild-type control (WT) and *tim23* mitochondria measured by $DiSC_3(5)$ (Sims et al., 1974). mito., mitochondria; val., valinomycin.

tim23-71,78, and *tim23-64,71,78* mitochondria, whereas they were imported into *tim23-64* and *tim23-78* mitochondria as efficiently as wild-type mitochondria (Fig. 2 and Fig. S1). In contrast, import of presequenceless polytopic inner membrane proteins, Tim23 and ADP/ATP carrier (AAC), via the TIM22 complex was not affected by the mutations of L64S, L71S, L78S, L71,78S, or L64,71,78S in the IMS domain of Tim23 (Fig. 2 and Fig. S1 A). Therefore, import of presequence-containing proteins via the TIM23 complex are impaired by the mutations in the Tim23 IMS domain, although import defects tend to be more pronounced for the matrix-targeted proteins than for the inner membrane–sorted proteins.

Mitochondria with mutations in the IMS domain of Tim50 are defective in protein import

We asked if mutations in the IMS domain of Tim50 that disrupt possible interactions with Tim23 in turn affect cell growth and protein import. On the basis of the analyses of Tim50 mutants with a deletion of predicted coiled-coil regions, we found that the coiled-coil regions 274–290 and 349–365 are important for Tim50 functions (unpublished data). We thus made *tim50* strains with mutations L279,282,286S (*tim50-279,282,286*) or A352S/F355S (*tim50-352,355*) (Fig. 3 A), and found that *tim50-279,282,286* cells, but not *tim50-352,355* cells, showed strong growth defects (Fig. 3 B). Mitochondria isolated from *tim50-279,282,286* cells exhibited the normal levels of translocator components and of $\Delta\Psi$ (Fig. 3, C and D).

We then conducted in vitro protein import into mitochondria with Tim50 containing the L279,282,286S or A352S/F355S mutation and obtained the results essentially similar to those for the Tim23 IMS domain mutant mitochondria. Import rates of matrix-targeted fusion proteins, pSu9-DHFR, pHsp60, $pb_2(167)\Delta$19-DHFR, and $pb_2(220)\Delta$19-DHFR, decreased for *tim50-279,282,286* mitochondria, but less significantly for *tim50-352,355* mitochondria (Fig. 3 E and Fig. S1 B). In contrast, although import of inner membrane–sorted fusion proteins, $pb_2(167)$-DHFR and $pb_2(220)$-DHFR, into *tim50-279,282,286* mitochondria was retarded, they were imported into *tim50-352,355* mitochondria nearly as efficiently as wild-type mitochondria (Fig. 3 E and Fig. S1 B). Import of Tim23 or ADP/ATP carrier (AAC) was not impaired by the L279,282,386S or A352S/F355S mutation (Fig. 3 E and Fig. S1 B).

Mutations in the coiled coils of Tim23 and Tim50 impair their interactions in the IMS

We analyzed the interactions between the IMS domains of Tim23 and Tim50 in the *tim23* and *tim50* mutant strains that are defective in cell growth and protein import in detail. First, we detected interactions of mutant Tim23 with wild-type Tim50 by coimmunoprecipitation of digitonin-solubilized mitochondria. The L71S mutation significantly reduced the amounts of Tim23 bound to Tim50FLAG and of Tim50 bound to Tim23 in *tim23-71*, *tim23-71,78*, and *tim23-64,71,78* mitochondria, whereas Tim23 bound to Tim50 was not reduced in *tim23-78* mitochondria or reduced partially in *tim23-64* mitochondria (Fig. 4, A and B). We obtained essentially the similar results by measuring binding of solubilized *tim23* mutant mitochondria to the recombinant IMS domain of Tim50 (Fig. 4 C) and by performing glycerol density-gradient centrifugation of solubilized *tim23* mutant mitochondria (Fig. S2 A, available at http://www.jcb.org/cgi/content/full/jcb.200808068/DC1). The reversed-charge mutant (*tim23-4K*) resulted in only moderate reduction of the amount of Tim50 bound to Tim23 (Fig. S2 B). We then analyzed interactions of mutant Tim50 with wild-type Tim23 by coimmunoprecipitation and found that the L279,282,386S mutation reduced the amounts of Tim50 bound to Tim23FLAG (Fig. 4 D), although glycerol density-gradient centrifugation was not sensitive enough to detect such reduced interactions (Fig. S2 C).

Downloaded from http://rupress.org/jcb/article-pdf/184/1/129/1562529/jcb_200808068.pdf by guest on 09 February 2026

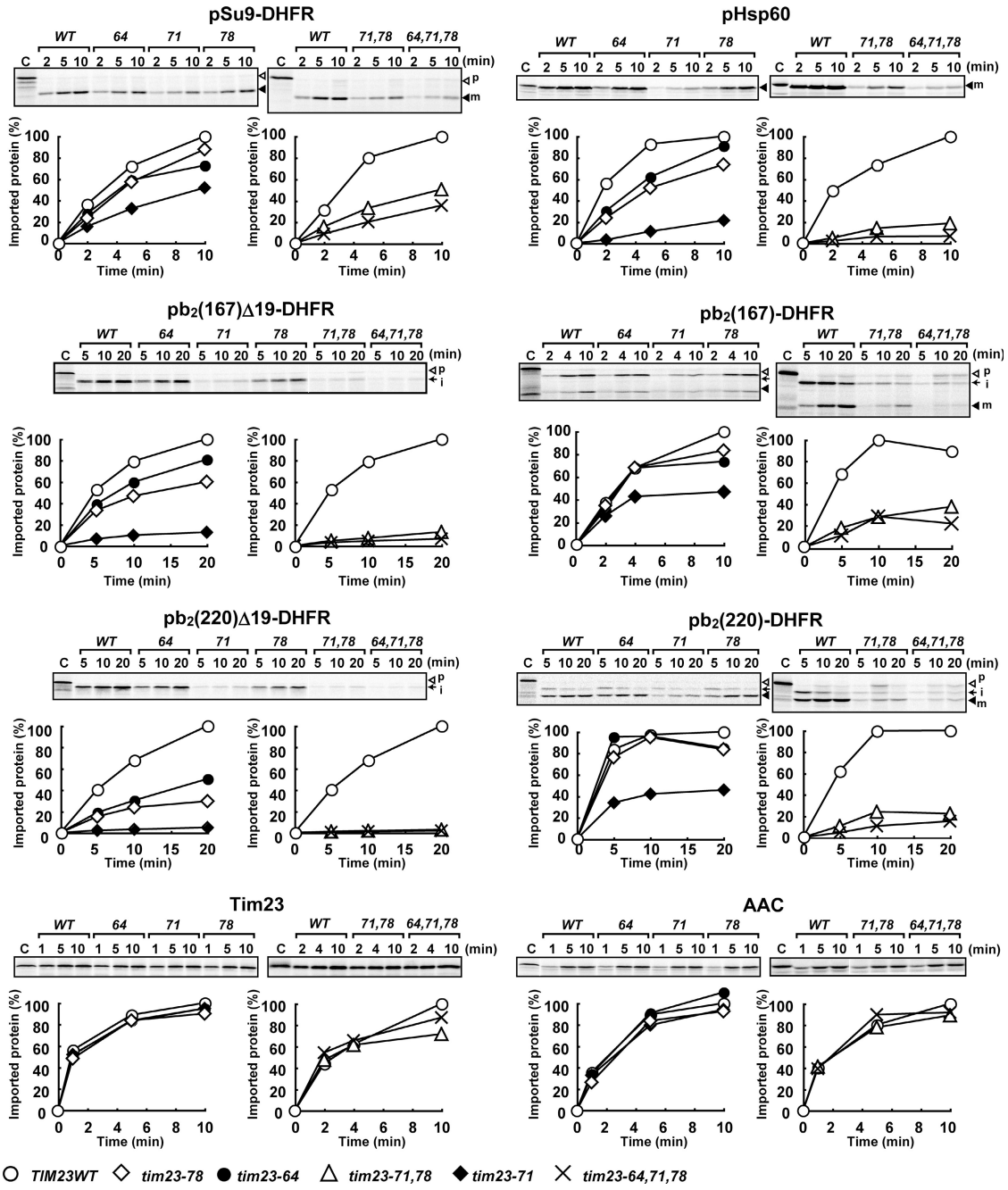

Figure 2. **Tim23 IMS domain mutants impair import into the matrix and sorting to the inner membrane differently.** Mitochondria were isolated from wild-type control (WT) and *tim23* mutant cells after cultivation in lactate medium at 30°C. Radiolabeled mitochondrial precursor proteins were incubated with those mitochondria at 30°C for indicated times. For quantification of the imported, protease-protected proteins, amounts of protease-resistant proteins in wild-type mitochondria after the longest incubation time were set to 100%. p, precursor form; i, processing-intermediate form; m, mature form.

To directly probe proteins interacting with the IMS domain of Tim23, we took the approach of site-specific photo-cross-linking. We incorporated a photoreactive unnatural amino acid, benzoylphenylalanine (BPA), into residue 64, 71, or 78 in Tim23 in vitro by the suppressor tRNA method (Kanamori et al., 1997, 1999). Tim23 with incorporated BPA was imported into isolated mitochondria and subjected to UV irradiation to trigger cross-linking of BPA with nearby proteins. Imported Tim23 was assembled into the TIM23 complex correctly as judged from blue native–PAGE analyses (Fig. S3 A, available at http://www.jcb.org/cgi/content/full/jcb.200808068/DC1) and introduction of BPA at, e.g., position 71 of Tim23 did not appear to disrupt the interaction with Tim50 completely. Cross-linked partners involving Tim23 were assigned to the subunits of the TIM23 complex or Tim14 (Fig. S3 B). BPA at positions 64, 71, and 78 was cross-linked to Tim50 and Tim17 (Fig. 4 E), confirming the proximity of these residues to Tim50. BPA at positions 71 and 78 was also cross-linked to Tim21 and BPA at residue 64 to Tim14 (Fig. 4 E), although Tim23 is not stoicheometrically saturated by these proteins (unpublished data). Therefore, the IMS domain of Tim23 is apparently in contact with multiple subunits of the TIM23 complex, yet coimmunoprecipitation with

Downloaded from http://rupress.org/jcb/article-pdf/184/1/129/1562529/jcb_200808068.pdf by guest on 09 February 2026

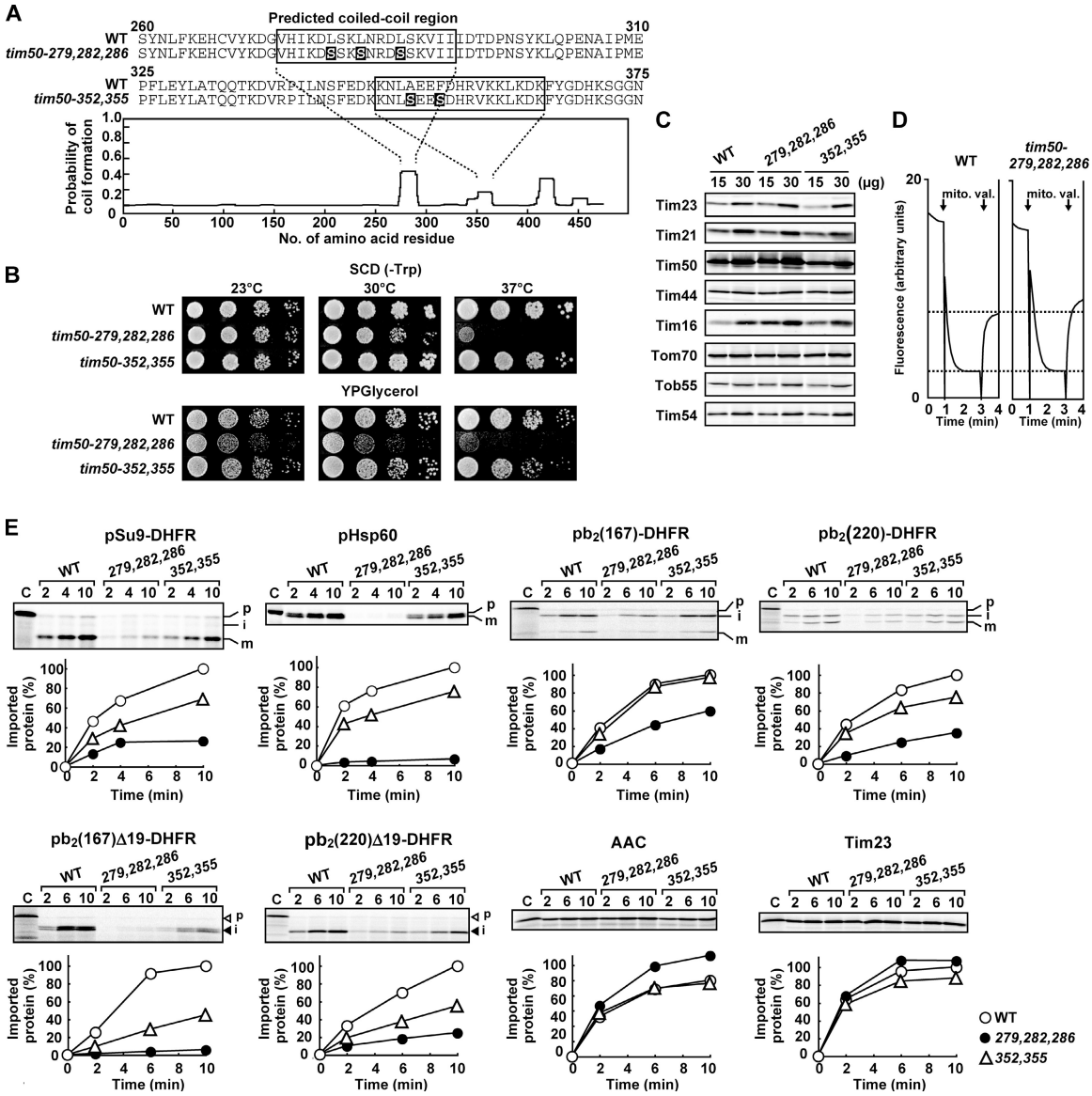

Figure 3. **Tim50 mutants with mutations in the coiled-coil region in the IMS.** (A) Amino acid sequences of the IMS domains of wild-type control (WT) and mutant Tim50 (top) and coiled-coil regions in Tim50 (bottom) predicted as in Fig. 1 A. Mutation points are shown in black. (B) Serial dilutions of wild-type and *tim50* mutant cells were plated on SCD (−Trp) and YPGlycerol and grown at the indicated temperature for 2 and 3 d, respectively. (C) Mitochondria were isolated from wild-type and *tim50* mutant cells grown at 23°C in lactate medium. Indicated amounts of mitochondrial proteins were analyzed for indicated proteins by SDS-PAGE followed by immunoblotting. (D) $\Delta\Psi$ of wild-type and *tim50-279,282,286* mitochondria measured as in Fig. 1 D. (E) Mitochondria were isolated from wild-type and *tim50* mutant cells after cultivation in lactate medium at 23°C. Radiolabeled precursor proteins were incubated with those mitochondria at 25°C for indicated times, and import reactions were analyzed as in Fig. 2. p, precursor form; i, processing-intermediate form; m, mature form.

tim23-64,71,78 mitochondria shows that mutations on the hydrophobic side of the coiled coil in Tim23 reduced the amount of bound Tim50, but not of bound Tim21, Tim14, or Tim17 (Fig. 4 F).

Tim23–Tim50 interactions in the IMS are important for presequence transfer from the TOM40 complex to the TIM23 complex

What are the roles of the coiled-coil interactions between Tim23 and Tim50 in the IMS in protein import? To address this question, we performed two-step import using *tim23* or *tim50* mutant mitochondria. In brief, we made use of an in vitro translocation intermediate of pSu9-DHFR generated in the absence of $\Delta\Psi$ at high temperature. This intermediate is arrested at the TOM40 complex in such a way that the presequence reaches the IMS side of the TOM40 complex, i.e., the trans site, whereas the DHFR domain is bound to the Tom40 channel in an unfolded state (Kanamori et al., 1999). The amount of the bound intermediate was not sensitive to salt concentrations and was not affected by the L64,71,78S or L279,282,286S mutation in the IMS domain of Tim23 or Tim50, respectively (Fig. 5 A, Binding). However, when we relieved the translocation arrest by replenishment of $\Delta\Psi$, efficiency in the chase into the matrix was reduced by both mutations (Fig. 5 A, Chase). These results show that Tim23–Tim50 interactions in the IMS affect the step after accumulation of the precursor protein at the trans site of the TOM40 complex.

Downloaded from http://rupress.org/jcb/article-pdf/184/1/129/1562529/jcb_200808068.pdf by guest on 09 February 2026

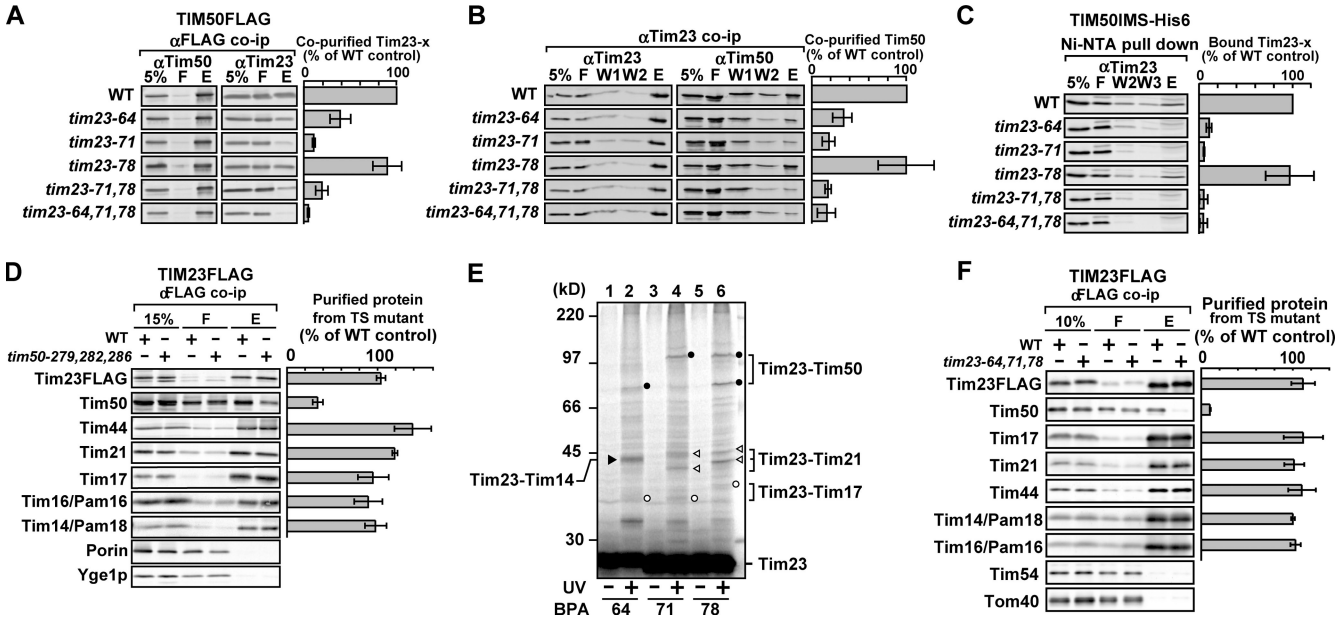

Figure 4. **Tim23 and Tim50 IMS domain mutants are defective in Tim23–Tim50 interactions.** (A) Wild-type control (WT) and *tim23* mutant mitochondria with FLAG-tagged Tim50 were solubilized with 1% digitonin and subjected to immunoprecipitation with the anti-FLAG antibody. 5%, 5% of the loaded proteins; F, 10% of unbound proteins; E, 100% of proteins eluted with 100 mM glycine-HCl, pH 2.5. (B) Immunoprecipitation was performed as in A (Tim50 is not FLAG tagged) using anti-Tim23 antibodies. (C) wild-type, *tim23-64*, *tim23-71*, *tim23-78*, *tim23-71,78*, *and tim23-64,71,78* mitochondria were solubilized with 0.5% Triton X-100 and subjected to incubation with Ni-NTA agarose loaded with purified recombinant Tim50 IMS. Bound proteins were eluted with 500 mM imidazole and analyzed by SDS-PAGE and immunoblotting with anti-Tim23 antibodies. 5%, 5% of the loaded proteins; FT, 10% of unbound proteins; W2-W3, 100% of washed fractions; E, 100% of eluted proteins. (D) Wild-type and *tim50* mutant mitochondria with FLAG-tagged Tim23 were solubilized with 1% digitonin and subjected to immunoprecipitation with the anti-FLAG antibody as in A. 15%, 15% of the loaded proteins; F, 10% of unbound proteins; E, 100% of eluted proteins. (E) Radiolabeled Tim23 with BPA incorporated at position 64, 71, or 78 was imported into mitochondria (W303-1A) at 25°C for 1 h and subjected to UV irradiation. Identified cross-linked partners are indicated. (F) Mitochondria with the FLAG-tagged version of Tim23 (WT) or L64,71,78S Tim23 (*tim23-64,71,78*) were solubilized with 1% digitonin and subjected to immunoprecipitation as in A. Error bars represent SDs from three independent experiments.

We then analyzed the effects of deteriorated Tim23–Tim50 interactions on the step of presequence transfer from the trans site to the TIM23 complex. Because a translocation intermediate lodged at the TOM40 complex in the absence of $\Delta\Psi$ is cross-linked to Tim50 (Yamamoto et al., 2002; Mokranjac et al., 2003), we asked by cross-linking experiments if Tim50 could receive the presequence from the trans site in *tim23* or *tim50* mutant mitochondria. pSu9-DHFR with BPA at position 21 in the presequence was accumulated at the TOM40 complex in the absence of $\Delta\Psi$. Subsequent UV irradiation yielded cross-linked products involving BPA at residue 21 with Tim50 as well as with Tom40 and Tom22 in wild-type mitochondria (Fig. 5 B). We found that the amounts of the cross-linked products between pSu9-DHFR and Tim50 significantly decreased in mitochondria with the mutation, L71S in Tim23 or L279,282,286S in Tim50 (Fig. 5 B). These results indicate that the Tim23–Tim50 interactions are important for efficient transfer of the presequence from the trans site of the TOM40 complex to Tim50, which likely reflects the Tim23-aided receptor ability of Tim50 for presequences as the import defects of *tim23-71* mitochondria were not resumed after rupturing the outer membrane (Fig. S3 C).

Tim23 and Tim50 physically link the TIM23 complex to the TOM40 complex

The efficient presequence transfer from the TOM40 complex to the TIM23 complex may be related to efficient recruitment of the TIM23 complex to the membrane contact sites and/or directly to the TOM40 complex. The former was proposed to involve penetration of the N-terminal 50 residues of Tim23 into the outer membrane (Donzeau et al. 2000; Vogel et al., 2006; Popov-Čeleketić et al., 2008), although such a role of Tim23 was questioned by others (Chacinska et al., 2003). The latter may be facilitated by direct interactions between the components of the TIM23 complex, including Tim21, and those of the TOM40 complex, including Tom22 (Chacinska et al., 2005; Mokranjac et al., 2005). We assessed possible effects of *tim23* or *tim50* mutations on the N-terminal interactions of Tim23 with the outer membrane by analyzing accessibility of the N terminus of Tim23 to the externally added protease (Donzeau et al., 2000; Yamamoto et al., 2002). The mutations L71S, L71,78S, and L64,71,78S in Tim23 and L279,282,286S and A352S/F355S in Tim50 indeed reduced the susceptibility of Tim23 to proteinase K (PK) added outside the mitochondria (Fig. 5 C). When we attached a folded protein A to the N terminus of Tim23, the N-terminal clipping of Tim23 by added PK was prevented (Fig. S4 A, available at http://www.jcb.org/cgi/content/full/jcb.200808068/DC1) as in the case of N-terminal 50-residue deletion of Tim23 (Donzeau et al., 2000). We then made *tim23* mutant strains expressing Tim23 with mutations that deteriorate its interactions with Tim50 as well as the deletion of the N-terminal 50 residues (Tim23Δ50) or N-terminal attachment of protein A (protein A–Tim23). Cells expressing

Downloaded from http://rupress.org/jcb/article-pdf/184/1/129/1562529/jcb_200808068.pdf by guest on 09 February 2026

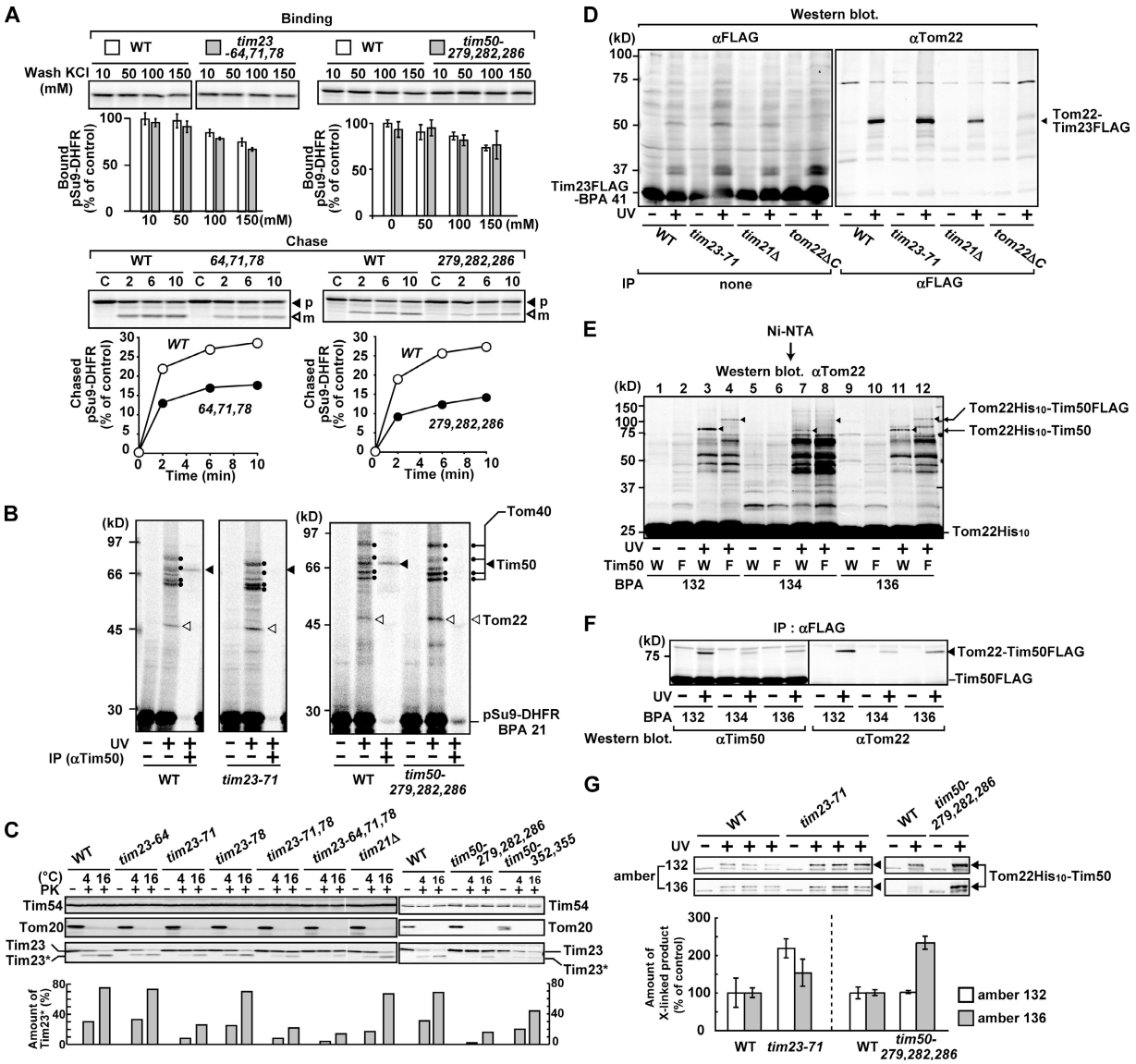

Figure 5. **Roles of Tim23–Tim50 interactions in the IMS in the early stage of protein translocation across the inner membrane.** (A, Binding) Radiolabeled pSu9-DHFR was incubated with CCCP-treated mitochondria isolated from wild-type control (WT), *tim23* mutant, and *tim50* mutant cells for 15 min at 30°C. Mitochondria were then washed with buffer containing indicated concentration of KCl, and bound proteins were analyzed by SDS-PAGE and radioimaging. (Chase) Mitochondria after binding of pSu9-DHFR in the presence of 100 mM KCl were incubated in chase buffer for indicated times (without following PK treatment). Proteins were analyzed by SDS-PAGE and radioimaging, and the chased, mature form was quantified. C, bound pSu9-DHFR (100%); p, precursor form; m, mature form. (B) Radiolabeled pSu9-DHFR containing BPA at position 21 was bound to wild-type control (WT), *tim23* mutant, and *tim50* mutant mitochondria in SM buffer with 10 mM KCl, 5 mM $MgCl_2$, and 2 mM methionine with 10 mg/ml valinomycin at 30°C for 15 min. Mitochondria were washed with SM buffer containing 150 mM KCl and kept on ice with (UV+) or without (UV−) UV irradiation in the same buffer for 5 min. The UV-irradiated mitochondria were solubilized and subjected to immunoprecipitation with anti-Tim50 antibodies (+IP), and proteins were analyzed by SDS-PAGE and radioimaging. Closed and open triangles indicate cross-linked products with Tim50 and Tom22, respectively. (C) Mitochondria isolated from wild-type, *tim23* mutant, *tim21*Δ, and *tim50* mutant cells were treated with 500 μg/ml PK for 20 min at 4 or 16°C. After stopping the reaction with 1 mM PMSF, the mitochondria were reisolated and proteins were analyzed by SDS-PAGE and immunoblotting with antibodies against Tim54 (with a domain exposed to the IMS), Tom20 (with a domain exposed to the cytosol), and Tim23. Total amounts of Tim23 and Tim23*, a protease-resistant fragment, are set to 100%. (D) Mitochondria isolated from indicated cells expressing Tim23FLAG with BPA at position 41 after UV irradiation (UV+) or mock treatment (UV−) were analyzed by SDS-PAGE and immunoblotting with the anti-FLAG antibody (left) or were subjected to immunoprecipitation with the anti-FLAG antibody, and Tom22 was detected by anti-Tom22 antibodies (right). (E) C-terminally $(His)_{10}$-tagged Tom22 with BPA at position 132, 134, or 136 was expressed in cells with either wild-type (W) or C-terminally FLAG-tagged (F) Tim50 and purified with Ni-NTA resin after UV irradiation (UV+) or mock treatment (UV−). The purified proteins were analyzed by SDS-PAGE and immunoblotting with anti-Tom22 antibodies. The weak bands above the cross-linked products (denoted with a closed triangle) are nonspecific bands. (F) Cell extracts were prepared from *TIM50FLAG/TOM22-BPA-X* (X = 132, 134, and 136) and were subjected to immunoprecipitation with the antibody against the FLAG epitope tag attached to the C terminus of Tim50. The purified proteins were analyzed by SDS-PAGE and immunoblotting with anti-Tim50 antibodies (left) and anti-Tom22 antibodies (right). (G) Tom22-$(His)_{10}$ with BPA at position 132 or 136 was expressed in *tim23-71*, *tim50-279,282,286*, or their corresponding wild-type cells and purified with Ni-NTA resin after UV irradiation (UV+) or mock treatment (UV−). Cross-linked products between Tom22 and Tim50 were detected by immunoblotting with anti-Tom22 antibodies and quantified with normalization by the total amount of authentic Tom22 plus Tom22-$(His)_{10}$. Amounts of the cross-linked products in corresponding wild-type cells were set to 100%. Error bars represent SDs from three independent experiments.

Downloaded from http://rupress.org/jcb/article-pdf/184/1/129/1562529/jcb_200808068.pdf by guest on 09 February 2026

Tim23Δ50 and protein A–Tim23 did not show significant growth defects at any temperature (Fig. S4, B and C). However, when combined with deteriorated Tim23–Tim50 interactions, the N-terminal 50-residue deletion of Tim23 in *tim23-64,71,78Δ50* and *tim23-71,78Δ50* strains and protein A attachment to Tim23 in *ProteinA-tim23-71* and *ProteinA-tim23-71,78* strains resulted in slower cell growth at elevated temperature than in cells expressing wild-type, full-length Tim23 (Fig. S4, B and C). Although *tim23-64* or *tim23-78* strains do not show obvious growth defects, even in combination with the N-terminal 50-residue deletion (Fig. 1 C and Fig. S4 B), attachment of protein A to expressed Tim23 with a mutation of L64S or L78S now exhibits synthetic growth defects (Fig. S4 C, bottom). These results suggest that the Tim23–Tim50 interactions facilitate the dynamic interactions of the N terminus of Tim23 with the outer membrane and/or TOM40 complex, which is important for vital cell growth, rather than mere stabilization of the interaction of Tim23 with the outer membrane.

We then probed possible transient interactions, if any, between the TIM23 and TOM40 complex, which would facilitate recruitment of the TIM23 complex to the TOM40 complex at contact sites, by site-specific photo-cross-linking in vivo (Chin et al., 2003). First, the *TIM23FLAG* gene with an amber codon for residue 41 of Tim23 was expressed in the yeast strain that contains an orthogonal pair of amber suppressor tRNA and its cognate aminoacyl-tRNA synthetase specific for BPA and UV irradiated. FLAG-tagged Tim23 and its cross-linked products were affinity purified and analyzed by SDS-PAGE. Tim23 with BPA at residue 41 generated a 50-kD cross-linked product, whose cross-linked partner was identified as Tom22 by immunoblotting with anti-Tom22 antibodies (Fig. 5 D) and by immunoprecipitation with anti-Tom22 antibodies followed by detection with the anti-FLAG antibody (not depicted). Because the 50-kD cross-linked product was not observed in mitochondria with Tom22 lacking the IMS domain (Fig. 5 D, *tom22ΔC*), residue 41 of Tim23 interacts with the IMS domain of Tom22. Second, when the *TOM22HIS10* gene with an amber codon for residue 132, 134, or 136 in the IMS domain of Tom22 was expressed in the same system, UV irradiation led to generation of 90-kD cross-linked products (Fig. 5 E, lanes 3, 7, and 11). These cross-linked products were found to involve Tim50 because they were shifted to 100 kD by attachment of the FLAG tag to Tim50 (Fig. 5 E, lanes 4, 8, and 12) and were detected by anti-Tom22 antibodies after affinity purification with the antibody against the FLAG epitope tag attached to the C terminus of Tim50 (Fig. 5 F, right). Thus, Tim23 and Tim50 are the first TIM23 components that can be cross-linked to the intact TOM40 complex even in the absence of translocating precursor proteins. Although the amounts of the cross-linked products between Tim23 and Tom22 were not affected by the L71S mutation in the Tim23 IMS domain (Fig. 5 D), those of the cross-linked products between Tim50 and Tom22 moderately increased with the mutation L71S in Tim23 or L279,282,286S in Tim50 (Fig. 5 G). Therefore, proper Tim23–Tim50 interactions facilitate dissociation of Tim50 from Tom22, likely resulting in efficient transfer of the presequence from the trans site of the TOM40 complex to Tim50.

Tim23–Tim50 interactions in the IMS facilitate the late step of protein translocation across the inner membrane

After presequence transfer from the TOM40 complex to Tim50, the precursor protein guided by the presequence has to enter the TIM23 channel. Gating of the TIM23 channel was proposed to involve Tim50-mediated Tim23 dimerization (Meinecke et al., 2006), and formation of the Tim23 dimer can be monitored by cross-linking of Tim23 (Bauer et al., 1996; Alder et al., 2008a) or by affinity copurification of Tim23 (Meinecke et al., 2006). However unexpectedly, although we confirmed that disuccinimidylglutarate generated a Tim23 dimer as a 50-kD cross-linked product (Fig. 6 A), the amount of the cross-linked product did not change with the mutations of L64S, L71S, L71,78S, or L64,71,78S in Tim23 (Fig. 6 A). We also found that imported Tim23, which was confirmed by blue native–PAGE to be correctly assembled into the TIM23 complex (not depicted), was coimmunoprecipitated with preexisting FLAG-tagged Tim23 (Fig. 6 B), yet the amounts of imported and coimmunoprecipitated Tim23 did not change with the L279,282,286S mutation in Tim50 (Fig. 6 B). Disrupted or weakened interactions between Tim23 and Tim50 in the IMS did not lead to reduced $\Delta\Psi$ (Fig. 1 D and Fig. 3 D) or impaired permeability barrier of the inner membrane, as well. These results suggest that the Tim23–Tim50 interactions in the IMS do not affect the dimer formation of Tim23, highlighting the apparently different effects of the Tim50 IMS domain between intact mitochondria and the reconstituted Tim23 system (Meinecke et al., 2006).

The Tim23–Tim50 interactions affect the matrix import and inner membrane sorting differently, the matrix import being more sensitive to the deteriorated Tim23–Tim50 interactions than the inner membrane sorting (Fig. 2, Fig. 3 E, and Fig. S1). These results suggest the possibility that, because matrix import requires multiple turnover of mtHsp70 as an import motor, motor functions of mtHsp70 in the matrix may be affected by the defects in Tim23–Tim50 interactions in the IMS. To assess the motor function of mtHsp70, we took advantage of the fact that the DHFR domain stabilized by its ligand methotrexate cannot go across the outer membrane, but instead forms a two-membrane–spanning intermediate that is closely apposed to the outer membrane by the motor function of mtHsp70. Such close apposition of the DHFR domain to the outer membrane is reflected in its resistance against externally added protease (Schwarz et al., 1993; Voisine et al., 1999). The presequence-cleaved mature form of the methotrexate-bound intermediate of $pb_2(220)\Delta19$-DHFR was PK resistant in wild-type mitochondria whereas it became PK sensitive in *tim23-64* and *tim23-78* mitochondria (Fig. 6 C). It should be noted that motor functions of mtHsp70 in *tim23-71* mitochondria was so defective that two-membrane–spanning intermediate could not be generated. Therefore the Tim23 mutations with defective Tim23–Tim50 interactions in the IMS apparently impair the motor function of mtHsp70 in the matrix.

To gain more insight into the impaired motor functions of mtHsp70 caused by deteriorate Tim23–Tim50 interactions, we analyzed the effects of overexpression of mtHsp70 on the *tim23* or *tim50* mutations. Overexpression of mtHsp70 from a multicopy

Downloaded from http://rupress.org/jcb/article-pdf/184/1/129/1562529/jcb_200808068.pdf by guest on 09 February 2026

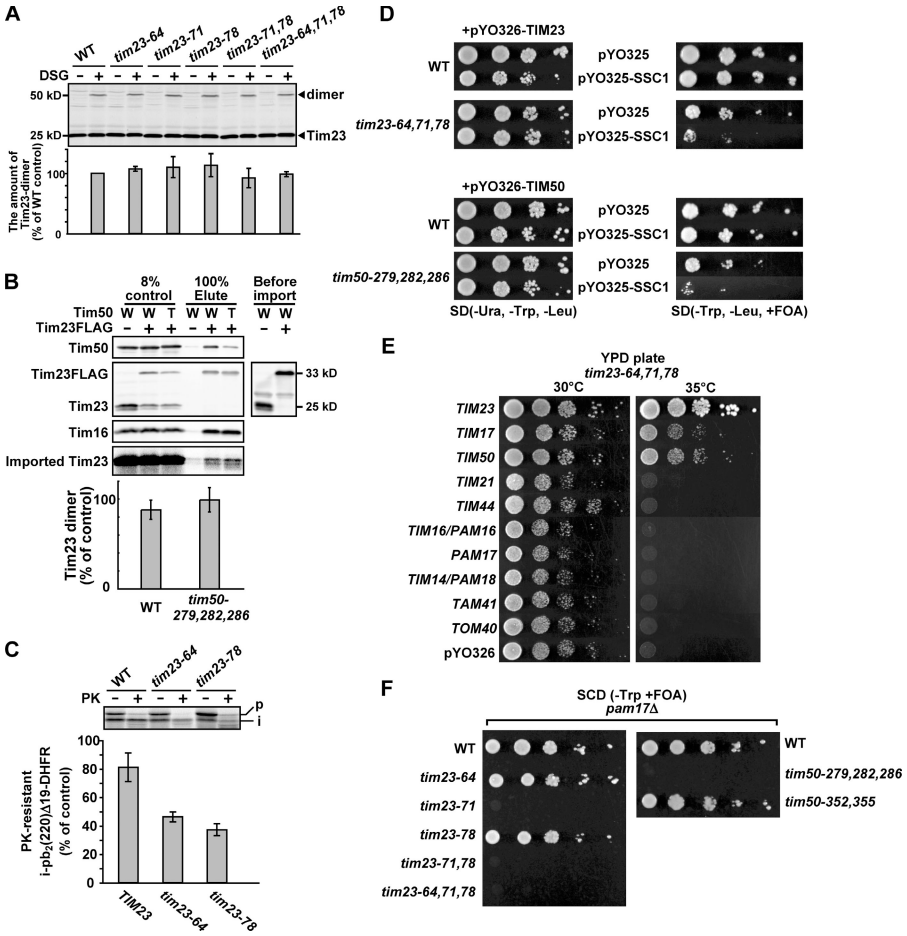

Figure 6. **Roles of Tim23–Tim50 interactions in the IMS in the late step of protein translocation across the inner membrane.** (A) Mitochondria isolated from wild-type control (WT), in which Tim23 is supplied from the plasmid, and *tim23* mutant cells were incubated in import buffer containing 0.05% BSA and 75 mM disuccinimidylglutarate on ice for 30 min. After quenching the reaction with 50 mM Tris-HCl, pH 7.4, Tim23 dimer formation was analyzed by SDS-PAGE followed by immunoblotting with anti-Tim23 antibodies. The amount of the Tim23 dimer in wild-type mitochondria was set to 100%. (B) Radiolabeled Tim23 was imported into wild-type mitochondria (WT) with or without Tim23FLAG and into *tim50-279,282,286* mitochondria (T) with Tim23FLAG for 20 min at 25°C and PK treated. The mitochondria was solubilized with 1.0% digitonin and subjected to coimmunoprecipitation with the anti-FLAG antibody. Proteins were analyzed by SDS-PAGE followed by radioimaging and immunoblotting with indicated antibodies before and after import. (C) Radiolabeled $pb_2(220)\Delta19$-DHFR was incubated with mitochondria for 20 min at 30°C in the presence of 10 mM methotrexate and 100 mM NADPH. The mitochondria were treated with 20 mg/ml PK for 20 min on ice. PK treatment was stopped by addition of 1 mM PMSF, and the mitochondria were reisolated by centrifugation. Proteins were analyzed by SDS-PAGE and radioimaging (top). The amounts of the PK-resistant processed intermediate (i) were quantified (bottom). The amounts of the processed intermediate without PK treatment are set to 100%. p, precursor form. (D) Serial dilutions of wild-type, *tim23*, and *tim50* mutant strains carrying yeast 2μ plasmid, pYO326-TIM23, and pYO325-SSC1 were plated on SD (−Ura, −Trp, −Leu; left) and SD (−Trp, −Leu, and +1 mg/ml 5′-fluoroorotic acid; right) and grown for 4 d at 23°C. (E) Serial dilutions of *tim23-64,71,78* carrying yeast 2μ plasmid (pYO326) encoding indicated genes were plated on YPD plates and grown for 2 d at 30 or 35°C. (F) Serial dilutions of *tim23* and *tim50* mutant strains lacking the *PAM17* gene with plasmid, pRS316-Tim23Δ50, and pRS316-Tim50, respectively, were plated on a SCD (−Trp and +FOA) plate. Error bars represent SDs from three independent experiments.

plasmid caused synthetic growth defects with *tim23-64,71,78* or *tim50-279,282,286* mutants (Fig. 6 D, right compared with left panels for the controls). This finding is in contrast to the cases of overexpression of other components of the TIM23 complex and MMC proteins; overexpression of Tim50 and Tim17 partly suppress the growth defects of the *tim23-64,71,78* mutant at elevated temperature (Fig. 6 E). These results suggest that the Tim23–Tim50 interactions in the IMS may thus facilitate turnover of mtHsp70 as an import motor; mtHsp70 overexpression will shift the equilibrium of mtHsp70 from the free state toward the TIM23 complex–bound state, thereby leading to synthetic growth defects with Tim23–Tim50 interaction mutants. Interestingly, we found synthetic growth defects of the coiled-coil mutants of Tim23 or Tim50 with deletion of the *PAM17* gene (Fig. 6 F). This suggests that Pam17 also facilitates the Tim23–Tim50–mediated activation of the motor functions of mtHsp70.

Discussion

Protein translocation across or insertion into the inner membrane can be dissected into three distinct steps (Fig. 7). In the first step, the presequences of both matrix-targeted and inner membrane–sorted precursor proteins are transferred from the trans site of the TOM40 complex to Tim50 of the TIM23 complex (Fig. 7, 1 → 2). In the second step, the presequence enters the TIM23 channel in a $\Delta\Psi$-dependent manner (Fig. 7, 2 → 3). This step also requires initial trapping of the presequence by the ATP-dependent motor mtHsp70 if translocation of the presequence through the TIM23 channel requires unfolding of the tightly folded passenger domain outside the mitochondria. In the third step, translocation of matrix-targeted proteins across the inner membrane further requires the motor function of mtHsp70 (and MMC proteins), which undergoes an ATP-dependent reaction cycle of holding on and off the incoming unfolded segment of precursor polypeptides at the outlet of the TIM23 channel (Fig. 7, 3 → 4-1), whereas insertion of inner membrane–sorted proteins into the inner membrane is independent of the function of mtHsp70 (Fig. 7, 3 → 4-2).

Here we found that the N-terminal region of Tim23 and the IMS domain of Tim50 directly interact with Tom22 in the absence of substrate precursor proteins. The Tim23–Tom22 and Tim50–Tom22 interactions may lead to efficient coupling of protein translocation through the TOM40 complex and TIM23

Downloaded from http://rupress.org/jcb/article-pdf/184/1/129/1562529/jcb_200808068.pdf by guest on 09 February 2026

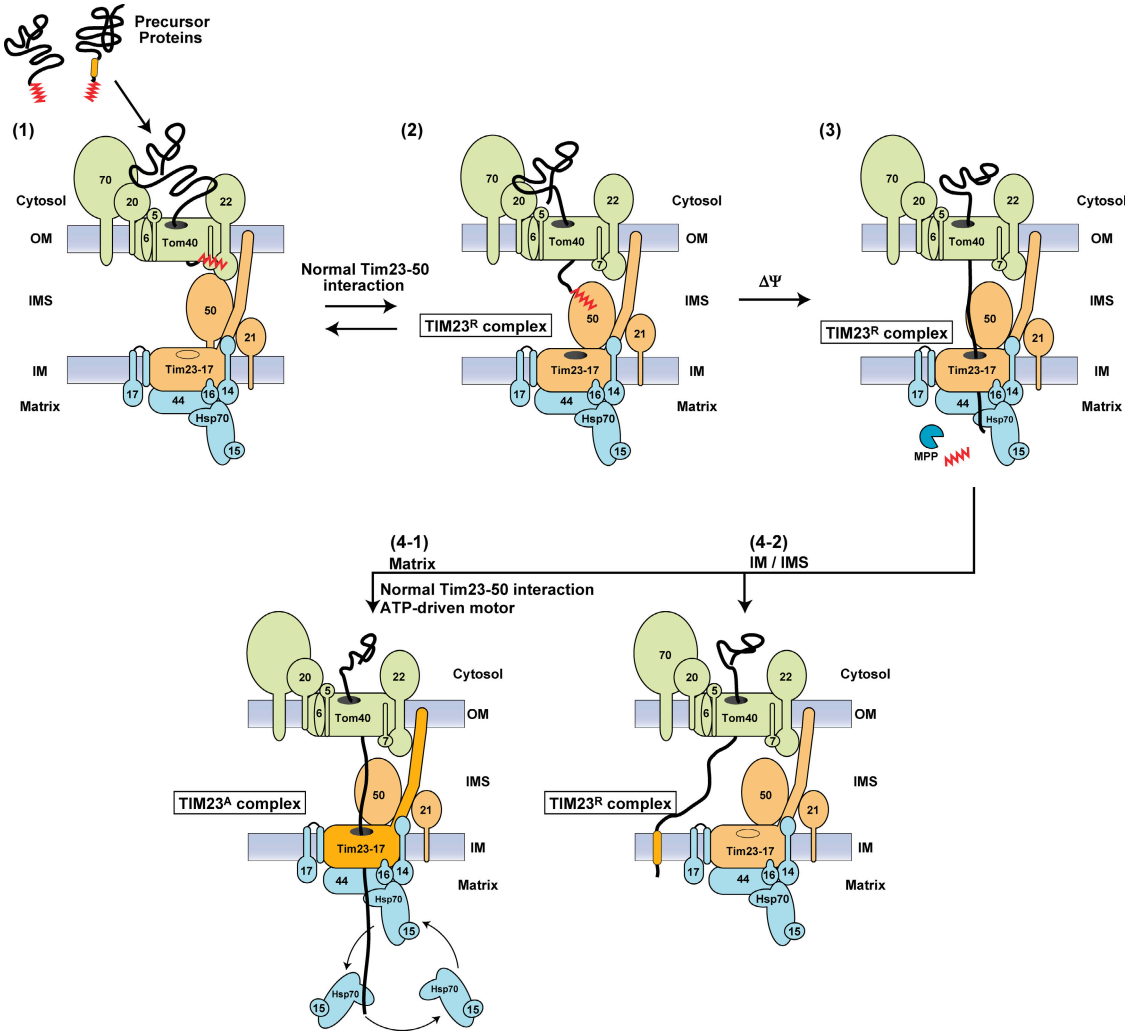

Figure 7. **A model of protein translocation across and insertion into the inner membrane via the TIM23 complex.** Note that the interactions among some of the components are dynamic rather than static.

complex. Although a similar function was suggested for Tim21 as well, interactions between Tim21 and Tom22 were found only after solubilization of mitochondrial membranes (Chacinska et al., 2005; Mokranjac et al., 2005) or only for high concentrations of purified recombinant proteins (Albrecht et al., 2006), but not in intact mitochondria (Chacinska et al., 2005; Mokranjac et al., 2005). We found here that the N-terminal interaction of Tim23 with the outer membrane (Fig. 5 C) or the contact between Tom22 and Tim23 (Fig. 5 D) was not altered by the absence of Tim21 and that depletion of Tim21 did not show synthetic growth defects with the *tim23* or *tim50* mutants (Fig. S4, D and E). Besides, the amount of the cross-linked product of the translocation intermediate at the TOM40 complex with Tim50 was not affected by depletion of Tim21 or by wash with 150 mM KCl (unpublished data), which abolishes interactions between Tim21 and Tom22 (Albrecht et al., 2006). Therefore, Tim21 does not appear to play a primary role in linking the TOM40 and TIM23 complexes.

Defects in the Tim23–Tim50 interactions caused by mutations in the Tim23 IMS domain are in the order of L71S > L64S >> L78S and those in the Tim50 IMS domain in the order of L279,282,286S > A352S/F355S. The normal Tim23–Tim50 interactions in the IMS appear to be important for the first step of the protein translocation because they facilitate efficient transfer of translocating proteins from the TOM40 complex to the TIM23 complex through transient interactions between the presequence and Tim50 (Fig. 5 A). Defective import of not only matrix-targeted proteins but also inner membrane–sorted proteins were observed for mitochondria containing the L71S mutation, but not the L64S or L78S mutation (Fig. 2); this suggests that the efficient protein transfer from the TOM40 to the TIM23 complex are impaired only when Tim23–Tim50 interactions are significantly disrupted. Because defects in Tim23–Tim50 interactions lead to the increased interaction between Tom22 and Tim50 (Fig. 5 G), Tom22 and presequences may compete with each other in interactions with Tim50. Proper Tim23–Tim50 interactions may well optimize the Tim50–Tom22 interactions so that Tim50 can stay close to Tom22 yet the presequence can efficiently substitute Tom22 to occupy Tim50 as well (Fig. 7, 1 → 2).

It was unexpected that changes in the Tim23–Tim50 interactions in the IMS did not affect the Tim23 dimer formation, which was proposed to reflect the channel closure, but instead

Downloaded from http://rupress.org/jcb/article-pdf/184/1/129/1562529/jcb_200808068.pdf by guest on 09 February 2026

affected the third step of the translocation of matrix-targeted proteins across the inner membrane. Defective motor functions of mtHsp70 usually cause retarded import of not only matrix-targeted proteins but also the inner membrane–sorted protein such as pb_2(220)-DHFR, but not pb_2(167)-DHFR (Voos et al., 1993). This is because pb_2(220)-DHFR, not pb_2(167)-DHFR, contains a tightly folded heme-binding domain (residues 81–181) downstream of the presequence (residues 1–80) and requires mtHsp70 for the second step or initial translocation of the N terminus of the presequence across the inner membrane (Glick et al., 1993). However, the effects of mutations L64S and L78S on the import rates of pb_2(220)-DHFR and pb_2(167)-DHFR do not markedly differ (Fig. 2), suggesting that the Tim23–Tim50 interactions do not affect binding of mtHsp70 in the second step of the TIM23 complex-mediated translocation. Rather, the Tim23–Tim50 interactions increase efficiency of mtHsp70 in the reaction cycle of binding to and release from the translocating protein in the third step of the inner membrane translocation. In other words, the Tim23–Tim50 interactions in the IMS facilitate turnover of mtHsp70 at the outlet of the TIM23 channel in the matrix (Fig. 7, 4-1). This interpretation was supported by the observation that overexpression of mtHsp70, which would hamper the mtHsp70 turnover, negatively affects the cell growth of *tim23* and *tim50* mutants (Fig. 6 D). It is to be noted that depletion of Tim50 leads to defects in the first and third steps of the TIM23 complex-mediated translocation (Geissler et al., 2002) like the *tim23* mutants with L64S or L78S mutation rather than L71S mutation. Besides, the *tim17-5* (Chacinska et al., 2005) and *tim23-76* mutant (van der Laan et al., 2007) were reported, which showed similar phenotypes, i.e., defects in only the third step of the TIM23 complex-mediated translocation (Chacinska et al., 2005). However, the defects in the motor function of mtHsp70 observed here are not caused by the lack of MMC proteins (Tim14 and Tim16) in the TIM23 complex because *tim23-64,71,78* and *tim50-279,282,286* mitochondria contain normal amounts of Tim14 and Tim16 (Fig. 4, C and E). Although we cannot rule out the possibility that the observed defects in motor functions are indirect consequences of the growth defects, a more likely explanation is that tertiary and/or quaternary structural changes of the TIM23 complex caused by defective Tim23–Tim50 interactions impaired the motor functions.

Chacinska et al. (2005) proposed that the TIM23 complex is in the equilibrium between the matrix translocation complex containing mtHsp70 and MMC proteins, but not Tim21, and the inner membrane–sorting complex containing Tim21 but not mtHsp70 or MMC proteins. However, this model was recently challenged by the observations that Tim21 was coimmunoprecipitated with MMC proteins (Tamura et al., 2006; Popov-Čeleketić et al., 2008). The previous observation that Tim21 was mutually exclusive with MMC proteins as a constituent of the TIM23 complex (Chacinska et al., 2005) may be explained by the findings that Tim21 and MMC proteins occupy only a fraction of the TIM23 core complex (Tim23 and Tim17) (unpublished data) and/or may be because of the artifact of using the protein A fusion protein of Tim21 (Popov-Čeleketić et al., 2008). The present study instead suggests that the TIM23 complex is in the two distinct states with or without activation for the successive action of the import motor mtHsp70 (Fig. 7). These two states of the TIM23 complex, the TIM23 complexes for motor activation ($TIM23^A$) and for motor resting ($TIM23^R$), may contain mtHsp70 and MMC proteins, but differ in their abilities to allow mtHsp70 to perform multiple rounds of holding on and off the incoming unfolded segments of translocating proteins. Conversion of the $TIM23^R$ complex to the $TIM23^A$ complex is caused by the Tim23–Tim50 interactions in the IMS, likely responding to the presence of precursor proteins in transit through the Tim23 channel, and is facilitated by Pam17. In other words, the IMS domains of Tim23 and Tim50 could monitor the presence of substrate polypeptide chains delivered from the TOM40 complex and transmit this information to the matrix side of the TIM23 complex, perhaps through Pam17, for on-demand activation of the motor functions without unnecessary idling. Evidently, future studies need to reveal the structural basis of the difference and of a switching mechanism between the $TIM23^R$ and $TIM23^A$ states.

Materials and methods

Plasmids and yeast strains

Yeast strains, plasmids, and primers used in this study are described in Table S1 (available at http://www.jcb.org/cgi/content/full/jcb.200808068/DC1). Gene disruption of the *TIM23* or *TIM21* gene and FLAG tagging of the *TIM23* gene were performed by homologous recombination using the PCR-mediated gene cassette. Introduction of the point mutations and amber codon into the *TIM23*, *TIM50*, or *TOM22* gene were performed by the overlap extension method using two pairs of primers or quick change.

Growth conditions

Cells were grown in YPD (1% yeast extract, 2% polypeptone, and 2% glucose), SD (0.67% yeast nitrogen base without amino acids and 2% glucose), SCD (0.67% yeast nitrogen base without amino acids, 0.5% casamino acid, and 2% glucose), or lactate (0.3% yeast extract, 0.1% glucose, 0.05% $CaCl_2$-H_2O, 0.05% NaCl, 0.06% $MgCl_2$-$6H_20$, 0.1% KH_2PO_4, and 2% lactic acid, pH 5.6) media with appropriate supplements. Cells that have the *kanMX4* gene were selected on YPD + G418 (1% yeast extract, 2% polypeptone, 2% glucose, and 500 µg/ml G418 sulfate). For plasmid shuffling to eliminate the *URA3*-containing plasmid, cells were grown on SCD (−Trp and +1 mg/ml 5′-fluoroorotic acid). For expression of BPA-containing Tim23FLAG, cells were grown in SD (−Trp, −Leu, and +1 mM BPA). Cells were grown in SD (−Trp, −Leu, and +1 mM BPA) for expression of Tim23FLAG with BPA and in SGal (−Trp, −Leu, and +1 mM BPA) or SGal (−Trp, −Leu, −Ade, and +1 mM BPA) for expression of Tom22 with BPA.

Import assays

Mitochondria were isolated from W303-1A, *tim21*Δ, and *tim23* mutant strains grown in lactate medium at 30°C and *tim50* mutant strains grown in lactate medium at 23°C. Radiolabeled precursor proteins were synthesized with rabbit reticulocyte lysate by coupled transcription/translation in the presence of [^{35}S]methionine. Mitochondria isolated from W303-1A, *tim21*Δ, and *tim23* and *tim50* mutant cells were incubated with radiolabeled precursor proteins in import buffer (250 mM sucrose, 10 mM MOPS-KOH, pH 7.2, 80 mM KCl, 2 mM KPi, 2 mM methionine, 5 mM dithiothreitol, 5 mM $MgCl_2$, 2 mM ATP, 2 mM NADH, and 1% BSA) at 30 or 25°C. The import reaction was stopped by addition of 10 µg/ml valinomycin. Protease treatment was performed by incubating the mitochondria with 100 µg/ml PK for 20 min on ice, which was inactivated by subsequent addition of 1 mM PMSF. The mitochondria were isolated by centrifugation, and proteins were analyzed by SDS-PAGE and radioimaging with a Storm 860 image analyzer (GE Healthcare) or Pharos FX Plus Molecular Imager (Bio-Rad Laboratories). Two-step import of pSu9-DHFR was performed essentially as described in Kanamori et al. (1999). In brief, radiolabeled

Downloaded from http://rupress.org/jcb/article-pdf/184/1/129/1562529/jcb_200808068.pdf by guest on 09 February 2026

pSu9-DHFR was incubated with mitochondria pretreated with 10 μM CCCP for 15 min at 30°C. Samples were diluted 11-fold with ice-cold SM buffer (250 mM sucrose and 10 mM MOPS-KOH, pH 7.2) containing different concentrations of KCl and incubated for 5 min on ice. The mitochondria were reisolated and used for chase experiments or analyzed by SDS-PAGE and radioimaging. For chase reactions, mitochondria were resuspended with chase buffer (250 mM sucrose, 10 mM MOPS-KOH, pH 7.2, 10 mM KCl, 5 mM $MgCl_2$, 10 mM DDT, 2% bovine serum albumin, 2 mM ATP, 2 mM KPi, 5 mM sodium malate, and 2 mM NADH) and incubated for indicated times at 25°C.

In vivo cross-linking

The plasmids for in vivo BPA cross-linking were provided by P.G. Schultz (The Genomics Institute of the Novartis Research Foundation, San Diego, CA). *GAL-TIM23/TIM23FLAG-BPA41* and its derivative cells were grown in SGal (−Trp and −Leu) to the saturated phase. To express Tim23FLAG containing BPA and to suppress expression of endogenous Tim23, cells were transferred to SD (−Trp, −Leu, +1 mM BPA) and grown to the log phase. *TOM22HIS10-BPA-X* and its derivative cells were grown in SD (−Trp, −Leu, and −Ade) to the saturated phase. For overexpression of Tom22-$(His)_{10}$ containing BPA, cells were transferred to SGal (−Trp, −Leu, −Ade, and +1 mM BPA) and grown to the log phase. BPA (BACHEM) was added to appropriate media heated at ~60°C from 1 M of stock solution in 1 M NaOH. During cultivations, cells were kept in the dark to prevent BPA from cross-linking reactions. Yeast cells were harvested, resuspended in water to 1.0 OD_{600} cells/ml, and divided into halves. One half was UV irradiated for 10 min at room temperature at a distance of 5 cm from a 365-nm UV lamp (22,000 μW/cm^2; B-100AP; UVP) and the other half was kept on ice.

Miscellaneous

Constructions of plasmids and yeast strains and yeast cell growth conditions are described in the online supplemental material. A binding assay using immobilized recombinant Tim50-IMS protein was performed as described previously (Geissler et al., 2002). Site-specific in vitro photo-cross-linking and immunoprecipitation were performed as described previously (Kanamori et al., 1999; Tamura et al., 2006). Immunoblotting was quantified with a Storm 860 image analyzer or Pharos FX Plus Molecular Imager.

Online supplemental material

Fig. S1 shows the quantification of the import rates of various mitochondrial proteins into the *tim23* or *tim50* mutant mitochondria with defective Tim23–Tim50 interactions. Fig. S2 shows the results of glycerol density gradient centrifugation for the TIM23 complex structures of the *tim23* mutant mitochondria with defective Tim23–Tim50 interactions. Fig. S3 shows the assignments of the cross-linked partners for Tim23 generated by site-specific photo-cross-linking. Fig. S4 shows that Tim23–Tim50 interactions facilitate dynamic assembly of the N terminus of Tim23 into the outer membrane. Table S1 shows the mutation points of the *tim23* mutants and sequences of the primers to construct various yeast mutant strains used in this study. Online supplemental material is available at http://www.jcb.org/cgi/content/full/jcb.200808068/DC1.

We thank Dr. Peter G. Schultz for the plasmids for in vivo BPA cross-linking. We thank Dr. K. Nakatsukasa and members of the Endo laboratory for discussions and comments.

We acknowledge support of this work by Grants-in Aid for Scientific Research of the Ministry of Education, Culture, Sports, Science and Technology and a grant from the Japan Science and Technology Agency. Y. Tamura was a research fellow and Y. Harada and K. Yamano are research fellows of the Japan Society for the Promotion of Science.

Submitted: 13 August 2008
Accepted: 9 December 2008

References

Albrecht, R., P. Rehling, A. Chacinska, J. Brix, S.A. Cadamuro, R. Volkmer, B. Guiard, N. Pfanner, and K. Zeth. 2006. The Tim21 binding domain connects the preprotein translocases of both mitochondrial membranes. *EMBO Rep.* 7:1233–1238.

Alder, N.N., J. Sutherland, A.I. Buhring, R.E. Jensen, and A.E. Johnson. 2008a. Quaternary structure of the mitochondrial TIM23 complex reveals dynamic association between Tim23p and other subunits. *Mol. Biol. Cell.* 19:159–170.

Alder, N.N., R.E. Jensen, and A.E. Johnson. 2008b. Fluorescence mapping of mitochondrial TIM23 complex reveals a water-facing, substrate-interacting helix surface. *Cell.* 134:439–450.

Bauer, M.F., C. Sirrenberg, W. Neupert, and M. Brunner. 1996. Role of Tim23 as voltage sensor and presequence receptor in protein import into mitochondria. *Cell.* 87:33–41.

Chacinska, A., P. Rehling, B. Guiard, A.E. Frazier, A. Schulze-Specking, N. Pfanner, W. Voos, and C. Meisinger. 2003. Mitochondrial translocation contact sites: separation of dynamic and stabilizing elements in formation of ta TOM-TIM-preprotein supercomplex. *EMBO J.* 22:5370–5381.

Chacinska, A., M. Lind, A.E. Frazier, J. Dudek, C. Meisinger, A. Geissler, A. Sickmann, H.E. Meyer, K.N. Truscott, B. Guiard, et al. 2005. Mitochondrial presequence translocase: switching between TOM tethering and motor recruitment involves Tim21 and Tim17. *Cell.* 120:817–829.

Chin, J.W., T.A. Cropp, J.C. Anderson, M. Mukherji, Z. Zhang, and P.G. Schultz. 2003. An expanded eukaryotic genetic code. *Science.* 301:964–967.

Donzeau, M., K. Káldi, A. Adam, S. Paschen, G. Wanner, B. Guiard, M.F. Bauer, W. Neupert, and M. Brunner. 2000. Tim23 links the inner and outer mitochondrial membranes. *Cell.* 101:401–412.

Endo, T., and D. Kohda. 2002. Functions of outer membrane receptors in mitochondrial protein import. *Biochim. Biophys. Acta.* 1592:3–14.

Endo, T., H. Yamamoto, and M. Esaki. 2003. Functional cooperation and separation of translocators in protein import into mitochondria, the double-membrane bounded organelles. *J. Cell Sci.* 116:3259–3267.

Esaki, M., T. Kanamori, S. Nishikawa, and T. Endo. 1999. Two distinct mechanisms drive protein translocation across the mitochondrial outer membrane in the late step of the cytochrome b_2 import pathway. *Proc. Natl. Acad. Sci. USA.* 96:11770–11775.

Esaki, M., H. Shimizu, T. Ono, H. Yamamoto, T. Kanamori, S. Nishikawa, and T. Endo. 2004. Mitochondrial protein import. Requirement of presequence elements and tom components for precursor binding to the TOM complex. *J. Biol. Chem.* 279:45701–45707.

Geissler, A., A. Chacinska, K.N. Truscott, N. Wiedemann, K. Brandner, A. Sickmann, H.E. Meyer, C. Meisinger, N. Pfanner, and P. Rehling. 2002. The mitochondrial presequence translocase: an essential role of Tim50 in directing preproteins to the import channel. *Cell.* 111:507–518.

Glick, B.S., A. Brandt, K. Cunningham, S. Muller, R.L. Hallberg, and G. Schatz. 1992. Cytochromes c_1 and b_2 are sorted to the intermembrane space of yeast mitochondria by a stop-transfer mechanism. *Cell.* 69:809–822.

Glick, B.S., C. Wachter, G.A. Reid, and G. Schatz. 1993. Import of cytochrome b_2 to the mitochondrial intermembrane space: the tightly folded heme-binding domain makes import dependent upon matrix ATP. *Protein Sci.* 2:1901–1917.

Kanamori, T., S. Nishikawa, I. Shin, P.G. Schultz, and T. Endo. 1997. Probing the environment along the protein import pathways in yeast mitochondria by site-specific photocrosslinking. *Proc. Natl. Acad. Sci. USA.* 94:485–490.

Kanamori, T., S. Nishikawa, M. Nakai, I. Shin, P.G. Schultz, and T. Endo. 1999. Uncoupling of transfer of the presequence and unfolding of the mature domain in precursor translocation across the mitochondrial outer membrane. *Proc. Natl. Acad. Sci. USA.* 96:3634–3639.

Koehler, C.M. 2004. New developments in mitochondrial assembly. *Annu. Rev. Cell Dev. Biol.* 20:309–335.

Komiya, T., S. Rospert, C. Koehler, R. Looser, G. Schatz, and K. Mihara. 1998. Interaction of mitochondrial targeting signals with acidic receptor domains along the protein import pathway: evidence for the 'acid chain' hypothesis. *EMBO J.* 17:3886–3898.

Kutik, S., B. Guiard, H.E. Meyer, N. Wiedemann, and N. Pfanner. 2007. Cooperation of translocase complexes in mitochondrial protein import. *J. Cell Biol.* 179:585–591.

Meinecke, M., R. Wagner, P. Kovermann, B. Guiard, D.U. Mick, D.P. Hutu, W. Voos, K.N. Truscott, A. Chacinska, N. Pfanner, and P. Rehling. 2006. Tim50 maintains the permeability barrier of the mitochondrial inner membrane. *Science.* 312:1523–1526.

Mokranjac, D., S.A. Paschen, C. Kozany, H. Prokisch, S.C. Hoppins, F.E. Nargang, W. Neupert, and K. Hell. 2003. Tim50, a novel component of the TIM23 preprotein translocase of mitochondria. *EMBO J.* 22:816–825.

Mokranjac, D., D. Popov-Čeleketić, K. Hell, and W. Neupert. 2005. Role of Tim21 in mitochondrial translocation contact sites. *J. Biol. Chem.* 280:23437–23440.

Neupert, W., and M. Brunner. 2002. The protein import motor of mitochondria. *Nat. Rev. Mol. Cell Biol.* 3:555–565.

Neupert, W., and J.M. Herrmann. 2007. Translocation of proteins into mitochondria. *Annu. Rev. Biochem.* 76:723–749.

Popov-Čeleketić, D., K. Mapa, W. Neupert, and D. Mokranjac. 2008. Active remodelling of the TIM23 complex during translocation of preproteins into mitochondria. *EMBO J.* 27:1469–1480.

Schatz, G., and B. Dobberstein. 1996. Common principles of protein translocation across membranes. *Science.* 271:1519–1526.

Downloaded from http://rupress.org/jcb/article-pdf/184/1/129/1562529/jcb_200808068.pdf by guest on 09 February 2026

Schwarz, E., T. Seytter, B. Guiard, and W. Neupert. 1993. Targeting of cytochrome b_2 into the mitochondrial intermembrane space: specific recognition of the sorting signal. *EMBO J.* 12:2295–2302.

Sims, P.J., A.S. Waggoner, C.-H. Wang, and J.F. Hoffman. 1974. Studies on the mechanism by which cyanine dyes measure membrane potential in red blood cells and phosphatidylcholine vesicles. *Biochemistry.* 13:3315–3330.

Tamura, Y., Y. Harada, K. Yamano, K. Watanabe, D. Ishikawa, C. Ohshima, S. Nishikawa, H. Yamamoto, and T. Endo. 2006. Identification of Tam41 maintaining integrity of the TIM23 protein translocator complex in mitochondria. *J. Cell Biol.* 174:631–637.

Truscott, K.N., P. Kovermann, A. Geissler, A. Merlin, M. Meijer, A.J. Driessen, J. Rassow, N. Pfanner, and R. Wagner. 2001. A presequence- and voltage-sensitive channel of the mitochondrial preprotein translocase formed by Tim23. *Nat. Struct. Biol.* 8:1074–1082.

van der Laan, M., A. Chacinska, M. Lind, I. Perschil, A. Sickmann, H.E. Meyer, B. Guiard, C. Meisinger, N. Pfanner, and P. Rehling. 2005. Pam17 is required for architecture and translocation activity of the mitochondrial protein import motor. *Mol. Cell. Biol.* 25:7449–7458.

van der Laan, M., M. Meinecke, J. Dudek, D.P. Hutu, M. Lind, I. Perschil, B. Guiard, R. Wagner, N. Pfanner, and P. Rehling. 2007. Motor-free mitochondrial presequence translocase drives membrane integration of preproteins. *Nat. Cell Biol.* 9:1152–1159.

Vogel, F., C. Bornhövd, W. Neupert, and A.S. Reichert. 2006. Dynamic subcompartmentalization of the mitochondrial inner membrane. *J. Cell Biol.* 175:237–245.

Voisine, C., E.A. Craig, N. Zufall, O. von Ahsen, N. Pfanner, and W. Voos. 1999. The protein import motor of mitochondria: unfolding and trapping of preproteins are distinct and separable functions of matrix Hsp70. *Cell.* 97:565–574.

Voos, W., B.D. Gambill, B. Guiard, N. Pfanner, and E.A. Craig. 1993. Presequence and mature part of preproteins strongly influence the dependence of mitochondrial protein import on heat shock protein 70 in the matrix. *J. Cell Biol.* 123:119–126.

Yamamoto, H., M. Esaki, T. Kanamori, Y. Tamura, S. Nishikawa, and T. Endo. 2002. Tim50 is a subunit of the TIM23 complex that links protein translocation across the outer and inner mitochondrial membranes. *Cell.* 111:519–528.

Yamano, K., M. Kuroyanagi-Hasegawa, M. Esaki, M. Yokota, and T. Endo. 2008. Step-size analyses of the mitochondrial Hsp70 import motor reveal the Brownian ratchet in operation. *J. Biol. Chem.* 283:27325–27332.

Downloaded from http://rupress.org/jcb/article-pdf/184/1/129/1562529/jcb_200808068.pdf by guest on 09 February 2026